Investigation of the methyl torsion in isotactic polypropylene — comparison between neutron inelastic scattering spectra and normal coordinate calculations

H. Takeuchi
Department of Chemistry, University of Tokyo, Japan*

and J. S. Higgins, A. Hill and A. Maconnachie
Department of Chemical Engineering, Imperial College, London, SW7 2AY, UK

and G. Allen and G. C. Stirling**
Science Research Council, Swindon, UK
(Received 6 February 1981)

Incoherent neutron scattering spectra for polypropylene and its partially deuterated analogue allow identification of the methyl torsion at 230 cm^{-1}. Comparison of the experimental spectra with the calculated densities of states shows discrepancies with the expected intensity of the methyl torsional band. Results from a stretch-oriented sample arranged so that the wave vector $\underline{Q}$ is first parallel ($\underline{Q}^{\parallel}$) and then perpendicular ($\underline{Q}^{\perp}$) to the helical chain axis indicate that the torsion is more intense and probably has a small frequency dispersion around 240 cm^{-1} for $\underline{Q}^{\parallel}$ and is weaker with a broad dispersion centred at 220 cm^{-1} for $\underline{Q}^{\perp}$.

Keywords Spectroscopy; inelastic neutron scattering; polypropylene; normal coordinate calculations; methyl torsion; orientation; density state

INTRODUCTION

The torsional and rotational motions of methyl side groups attached to polymeric chains are expected to produce intense features in neutron scattering spectra because they involve large amplitude motion of hydrogen[1]. In early experiments on polypropylene[2,3] very weak features observed in the region of 200 cm^{-1} were assigned to the torsional motion. It was suggested[2] that the methyl torsion was almost a free rotation at room temperature and above. However, the potential barrier associated with a methyl group having a fundamental torsion at 200 cm^{-1} is ~13 kJ mol^{-1} and the rotation would certainly not be free except at very high temperatures. Moreover, torsional vibrations have been shown subsequently to produce intense features in neutron spectra of a number of polymers[4,5]. A most notable example is poly(propylene oxide) where an intense peak at 228 cm^{-1} in the spectrum of the protonated sample is removed after deuteration of the CH_3 group[4].

These results make the weak torsional band observed for polypropylene very puzzling. In this paper we first identify the torsional peak in the neutron spectrum of polypropylene by specific deuteration of the polymer and then compare the spectra with calculations of the density of states from normal coordinate analysis. Finally the spectra from a highly stretch-oriented sample provide crucial information for explaining the low peak intensity from the torsional motion.

* At the time of this work: Department of Chemical Engineering, Imperial College, London SW7 2AY, UK
** Now at Unilever Research

EXPERIMENTAL

Materials

Isotactic polypropylene and the partially deuterated analogue $-(CD_2-\underset{\displaystyle CH_3}{\underset{|}{C}}D)_n-$ were prepared at UMIST by Dr P. Tait. The stretch-oriented sample and the sample of amorphous polypropylene were kindly lent by Dr H. A. Willis of ICI Plastics Division.

Neutron scattering experiment

The inelastic neutron scattering spectra were all obtained using the time-of-flight[1] spectrometers 6H[6a] and 4H5[6b] at AERE Harwell. The incident wavelength was 4.2 Å on the 6H and 4.5 Å on the 4H5 apparatus and spectra were obtained at scattering angles between 13° and 90° to the incident beam. The incident wavelength spread $\frac{\Delta\lambda}{\lambda}$ was 5%.

Sample films, 0.25 mm thick, were held in aluminium containers at 45° to the beam, unless otherwise specified. After corrections for background scattering and detector normalization data are obtained as the double differential cross-section with respect to neutron time of flight, τ, and the solid angle into which the neutron is scattered, Ω. This cross-section, $\partial^2\sigma/\partial\Omega\partial\tau$ is related to the amplitude

0032-3861/82/040499-06$03.00

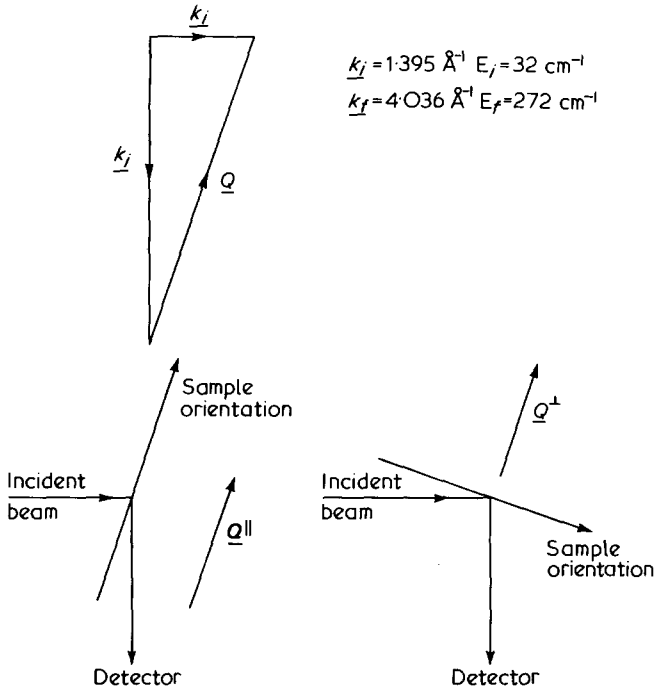

Figure 1 Diagrammatic representation of experimental sample orientation to obtain $\underline{Q}^{\parallel}$ and $\underline{Q}^{\perp}$

weighted density of states, $g(\omega)$ via[1,5,7]:

$$\frac{k_B T}{\hbar} g(\omega) = \rho(\omega) = \frac{\omega\hbar}{k_B T} \underset{|\underline{Q}^2|\to 0}{\mathrm{Lim}} \left[\frac{\exp(\hbar\omega/2k_B T)}{|\underline{Q}/^2} \frac{\hbar}{b^2} \frac{k_0}{k} \frac{\tau^3}{m} \frac{\partial^2\sigma}{\partial\Omega\partial\tau} \right] \tag{1}$$

where b is the scattering length of atom of mass m, and $\underline{k}_0$ and $\underline{k}$ are the incident and scattered neutron wave vectors respectively. $\hbar\underline{Q}$ is the momentum transfer or scattering vector defined by:

$$\underline{Q} = \underline{k} - \underline{k}_0$$

and $\hbar\omega$ is the energy transfer:

$$\hbar\omega = \varepsilon - \varepsilon_0 = \frac{h^2|k|^2}{2m} - \frac{h^2|k_0|^2}{2m}$$

Although the expression (1) for $\rho(\omega)$ contains contributions from all scattering centres, the presence of the b^2 term means that the cross-section, $\frac{\partial^2\sigma}{\partial\Omega\partial\tau}$ will be heavily weighted for motions involving atoms with large scattering amplitude, and notably for hydrogen modes for which b^2 is very large. The limit $|\underline{Q}|^2 \to 0$ is obtained by performing an extrapolation over points at corresponding energy transfers in spectra obtained at different angles of scattering. Where necessary an interpolation procedure is used to find suitable corresponding energy transfers.

In the case of the oriented samples only one experiment was possible with the correct orientation of the $\underline{Q}$ vector so that an extrapolation to zero $\underline{Q}$ was not possible. For these spectra an effective $\rho(\omega)$ was obtained using the same expression (1) without the limit $|\underline{Q}|^2 \to 0$. *Figure 1* shows a diagrammatic representation of the experimental layout and the corresponding wave-vector diagram used to obtain the two situations with momentum transfer parallel, $\underline{Q}^{\parallel}$, and perpendicular, $\underline{Q}^{\perp}$, to the direction of stretch.

NORMAL COORDINATE CALCULATIONS

Chain conformation and normal vibrations

Vibrations of a single polymer chain with a periodic structure are characterized by the phase difference, φ, between vibrational displacements of adjacent monomer units. Isotactic polypropylene forms a helix with three monomer units per translationally repeating unit in the crystalline state[9,10]. The line group of the single chain is 3_1 and the factor group is C_3. Vibrations with $\varphi = 0$ and $\varphi = 2\pi/3$ belong to the A and E species of C_3, respectively, and they are all optically (infra-red and Raman) active. Of the 27 A modes, one (ν_{26}) corresponds to the translation along the chain axis. The E modes are doubly degenerate and include two translations (ν_{27}) perpendicular to the chain axis.

In the crystalline state interchain interactions are expected to perturb the vibrations of a single chain. The unit cell of crystalline isotactic polypropylene consists of four helical chains parallel to the c axis. Some of the vibrational modes which correspond to translations or rotations in the single chain model become lattice (interchain) modes in the crystalline state. Effects of interchain interactions on intrachain vibrations can be estimated from band splittings of infra-red[11-13] and Raman[14,15] spectra. The splittings are very small or not observed, especially in the frequency range below 700 cm^{-1}, which indicates that the interchain forces are very small compared to the intrachain forces. Furthermore, the ambiguity in the chain directions of the four helices in the unit cell[9,10] prohibits appropriate evaluation of the interchain interactions in normal coordinate treatments.

Previous calculations

The vibrations of isotactic polypropylene have been treated in the single chain approximation mainly because of the reasons mentioned above. Miyazawa *et al.*[11a] calculated the frequencies of A and E modes for a single chain of hydrogenous polypropylene using a modified Urcy–Bradley force field. Snyder and Schachtschneider[16] made analogous calculations on hydrogenous and deuterated chains with a valence force field. Tadokoro *et al.*[13] also calculated the frequencies but they neglected the C–C skeletal and methyl torsions. Although Miyazawa's force field [11b] is based on only the infra-red data of the hydrogenous compound, it reproduces the infra-red and Raman frequencies of hydrogenous and deuterated polypropylene generally better than the other force fields.

Zerbi and Piseri[17] calculated the frequency dispersion curves and density of states for a single chain using the force field of Snyder and Schachtschneider. The calculated density of states was compared with the neutron spectrum observed by Safford *et al.*[2]. However, the comparison could not properly take account of relative peak intensities in the spectrum, because the calculated density of states was not weighted with the amplitudes of vibration.

Present calculations

The model used in this work is a single helix with 3_1 symmetry. Bond lengths and angles are those assumed by

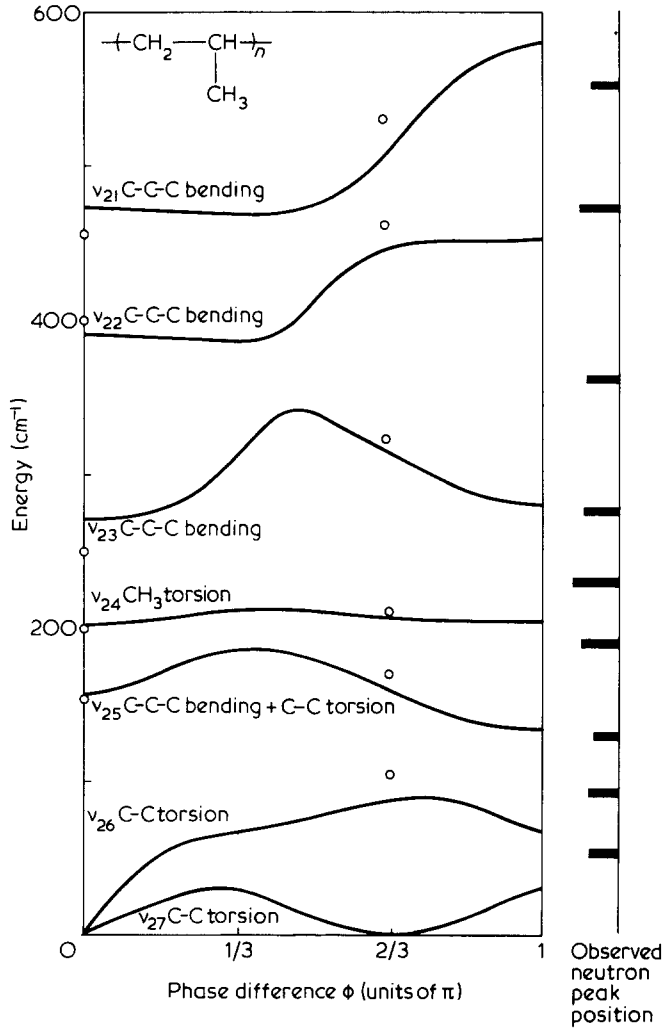

Figure 2 Dispersion curves calculated for $[CH_2CH.CH_3]_n$. Single isotactic chain. ○, observed infra-red frequencies[11b]

Miyazawa *et al.*[11a], r(C–C) = 1.54 Å, r(C–H) = 1.09 Å, and all the angles are tetrahedral. Using the force field of Miyazawa[11b] normal coordinate calculations were carried out for a range of φ between 0 and π. The dynamical matrix for each value of φ was constructed on the mass-weighted Cartesian displacement coordinates and was diagonalized to obtain normal frequencies and modes. *Figure 2* shows the calculated dispersion curves for a single chain of hydrogenous isotactic polypropylene. The circles in this Figure indicate observed infra-red frequencies from ref. 11. *Table 1* lists the infra-red and Raman frequencies from more recent experiments and compares them with the calculated frequencies of A and E modes. *Figure 3* shows the corresponding calculation for a partially deuterated chain together with some limited optical data from ref. 13.

For comparison with the neutron spectra the hydrogen-amplitude-weighted density of states $g_H(\omega)$ was calculated[18]:

$$g_H(\omega) = \frac{M}{3M_H N} \sum_H \sum_j \int_0^\pi d\varphi |A_j^H(\varphi)|^2 \delta[\omega - \omega_j(\varphi)] \qquad (2)$$

where N is a normalization constant chosen so that $\int g(\omega)d\omega$ equals the total number of normal modes in the frequency range. M_H is the mass of hydrogen and M that of a monomer unit. The subscript j denotes a specific branch of the dispersion curves. $A_j^H(\varphi)$ is the eigenvector element for a hydrogen atom expressed in terms of the atomic mass weighted Cartesian displacement coordinate. The sum Σ_H is made over all the H-atoms. The integration $\int_0^\pi d\varphi$ over the δ-functions $\delta(\omega - \omega_j(\varphi))$ was carried out using a linear extrapolation method[19,20]. Generalization of this method is described in ref. 21,

Table 1 $(CH_2CH.CH_3)_n$

	Observed				Calculated	
	Raman[14]		Neutron (stretched)			
I.r.[13]	298K	77K	∥	⊥	Optically active modes	A: $\phi = 0$ E: $\phi = 2\pi/3$
	53 m	58 m		55		ν_{27}
	65 sh	73 w				ν_{26}(A) or lattice?
	108 mb	102 m	100	100	90	ν_{26}(E)
		114 m				
			(145)		157	ν_{25}(A)
168⊥, vw	174 mb	170 sh		160	161	ν_{25}(E)
		177 m				
			195			
				220	203	ν_{24}(A)
			240		207	ν_{24}(E)
248∥, vw	253 w	251 w				
	260 w	267 w		290	272	ν_{23}(A)
318⊥, vw	318 wb	320 w			314	ν_{23}(E)
		326 w		350		
396∥, vw	400 m	400 m	400		391	ν_{22}(A)
452∥, vw		453 w			445	ν_{21}(A)
				450		
456⊥, vw	459 wb	460 w			473	ν_{22}(E)
528⊥, vw	529 wb	527.5 w	500		509	ν_{21}(E)
		533 w				

m = medium
w = weak
vw = very weak
sh = shoulder
b = broad

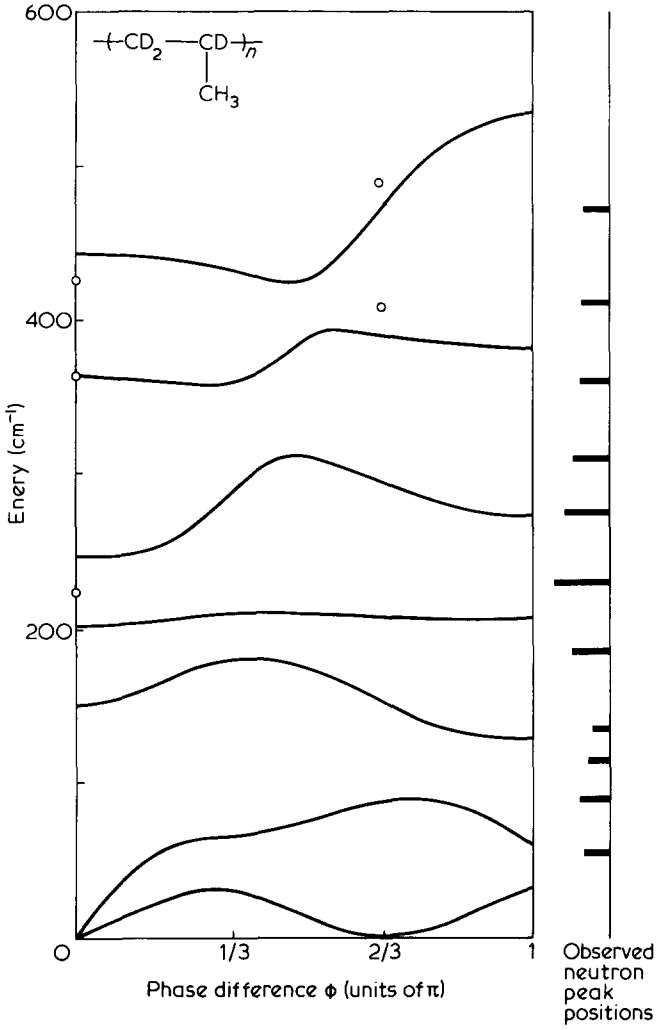

Figure 3 Dispersion curves calculated for $[CD_2CD.CH_3]_n$. Single isotactic chain. O, observed infra-red frequencies[13]. Assignment as in *Figure 2*

together with the algorithm used in the calculations. The whole range of phase differences from 0 to π was subdivided into 30 regions within each of which $\omega(\varphi)$ was assumed to be linear in φ. The width of the frequency channels was 0.2 cm^{-1}.

Figures 4a and *5a* show the calculated density of states for fully hydrogenous and partially deuterated chains. The effect of finite instrumental resolutions has been simulated by convoluting the calculated frequencies with a Gaussian energy spread of full width at half maximum equal to 10% of the neutron energy transfer.

DISCUSSION

Comparison of calculated spectra with neutron scattering results

Unoriented samples. Figures 4b and *5b* show the measured density of states for hydrogenous and partially deuterated chains for comparison with the corresponding calculated curves in *Figures 4a* and *5a*. *Figures 2* and *3* show the relevant peak frequencies as bars at the right-hand edge for comparison with calculation and with optical data. A qualitative agreement between the experimental and calculated spectra is seen above 300 cm^{-1}, though the resolution and statistics of the experimental data are not good enough to make a detailed comparison. Below 150 cm^{-1} the observed peak positions are higher by about 25 cm^{-1} than those calculated in the single chain approximation. The discrepancy may be caused by interchain forces, which usually tend to increase the frequency of intrachain modes, especially those at low frequency. The relative intensities in this frequency region seem to be rather well reproduced by the calculation.

The most intense bands observed for the hydrogenous (*Figure 4b*) and partially deuterated (*Figure 5b*) samples are both located at 230 cm^{-1}. The fact that the 230 cm^{-1} band does not shift and apparently gains relative intensity on deuteration of the backbone chain indicates that this band must be due to a vibration involving the CH_3 group predominantly. The spectrum of amorphous polypropylene (inset in *Figure 4b*) shows a strong and broad feature centred roughly around 240 cm^{-1}, suggesting that the vibration is a side chain rather than a backbone (crystalline) mode. Therefore, it is reasonable to assign this frequency to the CH_3 torsion. The calculation, on the other hand, predicts a very intense CH_3 torsional (ν_{24}) band at 205 cm^{-1}, a frequency lower than the experimental peak position. The disagreement in frequency is due to the fact that Miyazawa's force field, which was used in the present calculations, is based on the assignments of the CH_3 torsion frequencies to very weak infra-red bands at 200 and 210 cm^{-1}. (The torsional barrier is largely independent of the rest of the force field.)

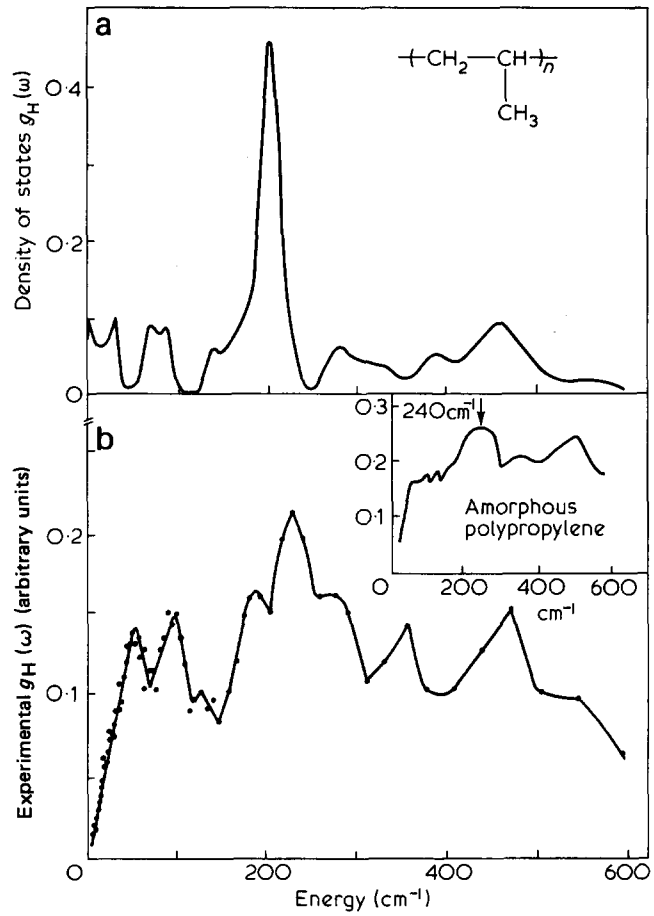

Figure 4 Hydrogen amplitude weighted density of states for $[CH_2CH.CH_3]_n$. (a) Calculated. (b) Observed. (Inset observed density of states for an amorphous sample)

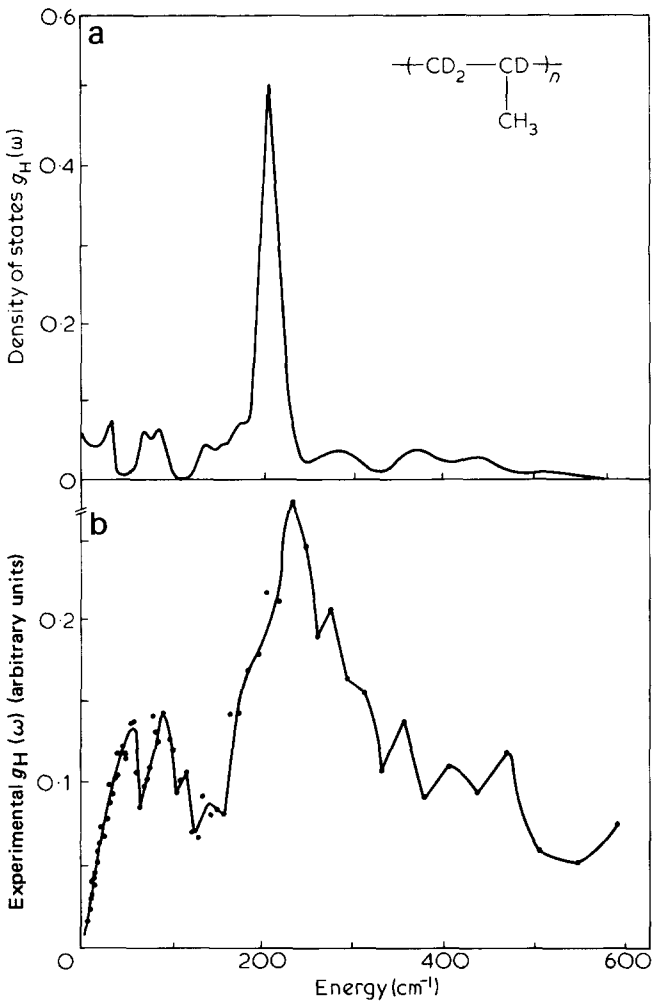

Figure 5 Hydrogen amplitude weighted density of states for $[CD_2CD.CH_3]_n$. (a) Calculated. (b) Observed

Since our neutron data locate the torsion around 230 cm^{-1} as described above, these infra-red bands might have other origins. Zerbi and Piseri[17] assumed an unusually large amplitude of vibration for the CH_3 torsion, because their calculation also predicted the torsion near 200 cm^{-1} but only a weak and broad feature had been observed at this frequency by Safford *et al.*[2]. It is noted that later infra-red studies[12,13] could not find any absorption around 200 cm^{-1}.

The calculated peak intensity of the torsional band is very high, whereas the experimental one is comparable with those of the other bands. It is not plausible that the intensity of the CH_3 torsion is distributed over the bands observed at 290 and 195 cm^{-1}, because these bands decrease in intensity on deuteration and are assigned to ν_{23} and ν_{25} from comparison with the calculated spectra. The relative weakness of the torsional band in the experimental spectrum will be discussed in the next section.

Oriented samples

In isotactic polypropylene, the C_3 axis of the methyl group projects outwards from the helical main chain backbone. This suggests two possible explanations for the weakness and breadth of the observed torsional mode. Interactions between chains may be enhanced by coupling of the methyl groups on adjacent chains leading to a large frequency dispersion for the methyl torsion in the direction perpendicular to the helical axis and a small dispersion parallel to the axis compared to the backbone modes in the corresponding directions. In the corresponding density of states spectra the methyl torsion would give a sharp intense peak when the $\underline{Q}$-vector is oriented parallel to the helical axis ($\underline{Q}^{\parallel}$) and a broad band for $\underline{Q}$ oriented in the perpendicular direction ($\underline{Q}^{\perp}$). A shift in peak frequency might also be expected. Alternatively, simple mechanical arguments suggest that the displacement of the protons is likely to be greater when the $\underline{Q}$-vector is parallel to the helical axis and therefore perpendicular to the torsion axis. This would also lead to a more intense band in the spectrum for $\underline{Q}^{\parallel}$ than for $\underline{k}^{\perp}$ *Figure 6* shows the experimental measurement of an effective density of states (equation (1) without the extrapolation to $\underline{Q}=0$) for the $\underline{Q}$-vector parallel and perpendicular to a stretch-oriented sample of isotactic polypropylene. If the relatively sharp band in the $\underline{Q}^{\parallel}$ spectrum at 240 cm^{-1} and the broad band for $\underline{Q}^{\perp}$ at 220 cm^{-1} are assigned to the torsional motion general agreement with the above predictions is found. The frequencies of the peak positions are listed in *Table 1* for comparison with calculation and with optical data. The frequency shift of the peak between $\underline{Q}^{\parallel}$ and $\underline{Q}^{\perp}$ spectra indicates that frequency dispersion is at least partially responsible for the weakness of the CH_3 torsion, since purely mechanical effects due to orientation of the methyl group would not be expected to introduce such a shift.

With the help of the calculated dispersion curves and displacement vectors for the hydrogen atoms, we can clarify the origins of bands below 200 cm^{-1} in the $Q^{\parallel}$ and $\underline{Q}^{\perp}$ spectra. The ν_{25} (C–C–C bending +C–C torsion) branch shows very little dispersion around $\varphi=\pi/3$ and $\varphi=\pi$, where the average hydrogen displacements are respectively nearly parallel and perpendicular to the chain axis. Therefore, the ν_{25} branch produces a parallel peak with $\varphi\sim\pi/3$ and a perpendicular one with $\varphi\sim\pi$. The observed $\underline{Q}^{\parallel}$ band at 195 cm^{-1} is assigned to the former peak and the $\underline{Q}^{\perp}$ band at 160 cm^{-1} to the latter. The 100

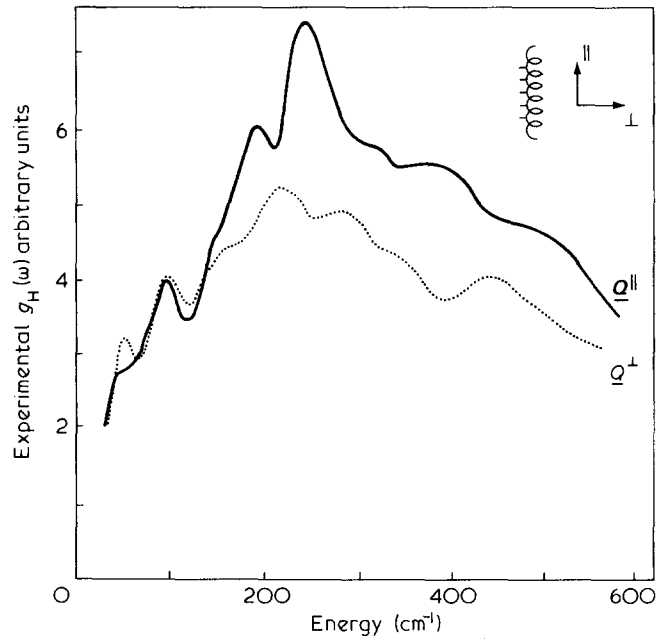

Figure 6 Effective density of states $\rho(\omega)$ observed for $\underline{Q}^{\parallel}$ and $\underline{Q}^{\perp}$ to the chain axis in stretch-oriented $[CH_2CH.CH_3]_n$

cm^{-1} band appearing in both the $\underline{Q}^{\parallel}$ and $\underline{Q}^{\perp}$ spectra is attributed to part of the ν_{26} (C–C torsion) branch with $\varphi > \pi/3$. Calculations predict a mixed polarization for this branch in that range of φ. The band at 55 cm^{-1} loses most of its intensity in the $\underline{Q}^{\parallel}$ spectrum. Since this band is also found for the amorphous sample, we assign it to the lowest-frequency branch, ν_{27} (C–C torsion), of the intrachain modes. The displacement of the ν_{27} vibration is polarized almost perpendicularly to the chain axis as expected from the fact that this branch corresponds to the overall rotation about the chain axis at $\varphi = 0$ and translations perpendicular to the axis at $\varphi = 2\pi/3$ in the single chain approximation. This explains the relatively high intensity of the 55 cm^{-1} band in the $\underline{Q}^{\perp}$ spectrum.

CONCLUSION

The methyl torsion has a small frequency dispersion around 240 cm^{-1} in the direction parallel to the chain axis and a broad dispersion centred at 220 cm^{-1} in the perpendicular direction. The average value of 230 cm^{-1} is observed in both hydrogenous and partially deuterated unoriented samples. Although Miyazawa *et al.*[11a] assigned two very weak i.r. absorptions at 200 and 210 cm^{-1} (not observed in later experiments) to the methyl torsion, the neutron scattering data clearly indicate a reassignment of the methyl torsional mode to 230 cm^{-1}. The relatively broad dispersion due to interchain interactions explains the low intensity of the methyl torsional band in unoriented samples of isotactic polypropylene.

REFERENCES

1 Allen, G. and Higgins, J. S. *Rep. Prog. Phys.* 1973, **36**, 1073 **36**, 1073
2 Safford, G. J., Danner, H. R., Boutin, H. and Berger, M. *J. Chem. Phys.* 1964, **40**, 1426
3 Yasukawa, T., Kimura, M., Watanabe, N. and Yamada, Y. *J. Chem. Phys.* 1971, **55**, 983
4 Higgins, J. S., Allen, G. and Brier, P. N. *Polymer* 1972, **13**, 157
5 Allen, G., Wright, C. J. and Higgins, J. S. *Polymer* 1974, **15**, 319
6a 'Dido 6H long wavelength neutron spectrometer' L. J. Bunce, D. H. C. Harris and G. C. Stirling, AERE R6246 (1970)
6b 'Neutron Beam Instruments at Harwell' A. H. Baston and D. H. C. Harris, AERE R9278 (1978)
7 Howard, J. and Waddington, T. C. in 'Advances in Infra-red and Raman Spectroscopy' (Eds. R. J. H. Clark and R. E. Hester) Vol 7, Heyden, London, 1980
8 Baston, A. H. 'The collection and processing of data from three time of flight spectrometers', AERE M2570 (1972)
9 Natta, G. and Corradini, P. *Supplimento al Vol. XV, Serie X del Nuovo Cimento* 1960, **N1**, 40
10 Mencik, Z. *Macromol. Sci. Phys.* 1972, **B6**, 101
11a Miyazawa, T., Fukushima, K. and Ideguchi, Y. *J. Polym. Sci., Part B* 1963, **1**, 385
11b Miyazawa, T. *J. Polym. Sci., Part C*, 1963, 59
12 Goldstein, M., Seelig, M. E., Willis, H. A. and Zichy, V. J. I. *Polymer* 1973, **14**, 530
13 Tadokoro, H., Kobayashi, M., Ukita, M., Yasufukum, K. and Murahashi, S. *J. Chem. Phys.* 1965, **42**, 1432
14 Fraser, G. V., Hendra, P. H., Watson, D. S., Gall, M. J., Willis, H. A. and Cudby, M. E. A. *Spectrochim. Acta* 1973, **29A**, 1525
15 Balley, R. T., Hyde, A. J. and Kim, J. J. *Spectrochim. Acta* 1974, **30A**, 91
16 Snyder, R. G. and Schachtschneider, J. H. *Spectrochim. Acta* 1964, **20**, 853
17 Zerbi, G. and Piseri, L. *J. Chem. Phys.* 1968, **49**, 3840
18 Reynolds, P. A., Kjems, J. K. and White, J. W. *J. Chem. Phys.* 1972, **56**, 2928
19 Gilat, G. and Raubenheimer, L. J. *Phys. Rev.* 1966, **144**, 390
20 Raubenheimer, L. J. and Gilat, G. *Phys. Rev.* 1967, **157**, 586
21 Takeuchi, H. *PhD Thesis*, University of Tokyo, 1976